AJNR

Dyke Award. Europium-DTPA: a gadolinium analogue traceable by fluorescence microscopy.

A D Elster, S C Jackels, N S Allen and R C Marrache

AJNR Am J Neuroradiol 1989, 10 (6) 1137-1144
http://www.ajnr.org/content/10/6/1137

Dyke Award

Europium-DTPA: A Gadolinium Analogue Traceable by Fluorescence Microscopy

Allen D. Elster[1]
Susan C. Jackels[2]
Nina S. Allen[3]
Ron C. Marrache[2]

A lanthanide series chelate, europium(Eu)-DTPA, was synthesized to serve as a histochemical analogue for the widely used MR contrast agent gadolinium(Gd)-DTPA. Eu and Gd, being neighboring elements on the periodic table, share many fundamental properties, including ionic radius, valence, and chemical reactivity. Eu-DTPA, however, possesses one important physical property not shared by Gd-DTPA: luminescence under ultraviolet light. The feasibility of detecting Eu-DTPA in animal tissues under fluorescence microscopy was systematically evaluated and documented.

Distinctive orange-red luminescence of Eu-DTPA could be observed in the kidneys, livers, dura, choroid, and pituitary glands of rats after intravascular injection. No luminescence was detected in areas of brain beyond an intact blood-brain barrier. When the brain was locally injured by an experimental laceration, however, leakage of Eu-DTPA was detected. Electron probe microanalysis confirmed the parallel presence or absence of simultaneously injected Eu-DTPA and Gd-DTPA in all tissues studied. Fluorescence microscopy with Eu-DTPA has thus been validated as a method for tracing the distribution of Gd-DTPA at the microscopic level.

***AJNR* 10:1137–1144, November/December 1989**

The recent development of paramagnetic MR contrast agents such as gadolinium (Gd)-DTPA has been received by the radiologic community with justifiable enthusiasm. Like their iodinated counterparts in CT, MR contrast agents appear to offer increased sensitivity and specificity for detecting and characterizing a number of diseases affecting the nervous system [1–11]. While there is great interest in these compounds from a clinical and radiologic viewpoint, relatively little is known about their distribution or dynamics at the cellular level.

It has been generally assumed that Gd-DTPA and other soluble MR contrast agents distribute similarly to those used in CT: they do not cross an intact blood-brain barrier and diffuse in the extracellular spaces around lesions [12–25]. While this concept appears valid in the broad sense, it is supported only by limited experimental data. No satisfactory methods presently exist for localizing or tracing Gd-DTPA in tissue specimens at the cellular level.

The purpose of this research was to develop an analogue of Gd that could be directly visualized in fresh or frozen tissue by light microscopy. Europium (Eu) was chosen for this purpose since it occupies a position on the periodic table adjacent to Gd and many of its physical properties are similar (Table 1). Because the charge and ionic radii of Eu and Gd are nearly the same, Eu and Gd complexes should be expected to have nearly identical solubilities, molecular weights, charges, and tissue distributions. However, by virtue of a slightly different inner electron structure, Eu compounds possess one important physical property not shared by those of Gd, luminescence under ultraviolet (UV) light [26]. We hypothesized that Eu-DTPA could be used as a close chemical analogue of Gd-DTPA and could be visualized in tissue by fluorescence microscopy. To demonstrate the analogous behavior of Eu- and Gd-DTPA in vivo we also endeavored to validate the parallel distributions

Received March 16, 1989; revision requested June 5, 1989; revision received June 19, 1989; accepted July 3, 1989.

Presented at the annual meeting of the American Society of Neuroradiology, Orlando, March 1989.

This work was supported in part by a grant from Forsyth Cancer Service, Inc.

[1] Department of Radiology, The Bowman Gray School of Medicine, Wake Forest University, 300 S. Hawthorne Rd., Winston-Salem, NC 27103. Address reprint requests to A. D. Elster.

[2] Department of Chemistry, The Bowman Gray School of Medicine, Winston-Salem, NC 27103.

[3] Department of Biology, The Bowman Gray School of Medicine, Winston-Salem, NC 27103.

0195-6108/89/1006–1137

TABLE 1: Physical Similarities of Eu and Gd*

Physical Property	Europium (Eu)	Gadolinium (Gd)
Atomic number	63	64
Atomic weight (g/mol)	151.96	157.25
Electronic configuration	$4f^7 5d^0 6s^2$	$4f^7 5d^1 6s^2$
Atomic radius (pm)	185	180
Ionic radius (+3 state, pm)	95.0	96.8
Principal valance	+3	+3

* Data from [32].

of the two compounds in various tissue specimens by electron probe microanalysis.

Materials and Methods

Reagents

Eu-DTPA was prepared in our laboratory in a manner similar to that for Gd-DTPA described by Weinmann et al. [27]. Europium oxide* was mixed with diethylenetriaminepentaacetic acid† in distilled water in a 1:2 molar ratio. The solution was heated to 85°C for 3 hr with constant stirring. The pH of the solution was then adjusted to 7.0 by the addition of concentrated NaOH. Distilled water was added to bring the solution to a concentration of 0.5 mol/l Eu-DTPA. Crystalline Eu-DTPA was obtained by sequentially treating the concentrated solution with acetone and absolute ethanol, then suction filtering it through a Millipore filter.

Gd-DTPA solution at a concentration of 0.5 mol/l was obtained commercially.‡ Gd-DTPA crystals were prepared from Gd_2O_3 in a manner similar to that described above for crystallization of Eu-DTPA.

Animals

Mature male Fisher 344 rats weighing approximately 300 g each were used exclusively for the experiments. Anesthesia induction was performed with an inhalational agent (methoxyflurane). Maintenance anesthesia was provided by periodic intraperitoneal injections of ketamine (25 mg/kg) and xylazine (2 mg/kg). Intravascular injections of saline, Eu-DTPA, or Gd-DTPA were made in selected animals via direct cardiac puncture with a 25-gauge needle. All animals were sacrificed by guillotining while under general anesthesia. The brains and other organs were rapidly removed and examined by fluorescence microscopy or electron probe microanalysis.

An initial group of three rats served as controls. They received intracardiac injections of normal saline (0.5 ml) only. Small cubes (approximately 1 mm^3) of their brains were harvested and soaked in various dilutions of Eu-DTPA and Gd-DTPA. These soaked tissue specimens were then used to calibrate and establish sensitivities for the detection of Eu and Gd by fluorescence microscopy and electron probe microanalysis.

A second group of six rats received intracardiac injections of Gd-DTPA (0.1 mmol/kg), Eu-DTPA (0.1 mmol/kg), or both (Gd-DTPA and Eu-DTPA, 0.1 mmol/kg each). They were sacrificed approximately 5–10 min after injection. Specimens of liver, spleen, kidney, muscle, dura, optic nerve, pituitary, choroid, frontal lobe, cerebellum, and pons were rapidly obtained and sectioned by hand under a ×20 dissecting microscope. These specimens were then subjected to fluorescence microscopy or electron probe microanalysis.

A third group of three rats received an experimental brain laceration 1 hr prior to injection. This was performed by advancing a high-speed dental drill through the calvarium into the brain. Under general anesthesia the skin and pericranial soft tissues were stripped locally from the skull near its vertex. A site 10 mm behind the interorbital line and 3 mm to the right of midline was chosen for drill insertion. A high-speed dental drill fitted with a 1/16-in. bit was advanced vertically through the calvarium and into the brain approximately 3–5 mm. The drill was then withdrawn and the soft tissues closed over the skull defect. The above technique was found to produce reliably a vertically oriented laceration in the posterior portion of the right frontal lobe with little damage to the surrounding brain (Fig. 1). One hour after the production of this laceration the rats were injected intravascularly with saline, Gd-DTPA, and Eu-DTPA, or both as before. A specimen of brain including the injured region was then examined by fluorescence microscopy and electron probe microanalysis for the presence of Gd or Eu at the site of blood-brain barrier and vascular disruption.

Fluorescence Microscopy

Fluorescence microscopy of fresh, unfixed specimens was performed on an Axiophot system§ equipped with Plan-Neofluor objective lenses (×20, ×40, ×100). A specifically designed filter set transmitted the incident UV light and allowed visualization of the red-range fluorescence of Eu-DTPA (Fig. 2). This included a UV excitation filter (360–440 nm), a midrange dichroic mirror (460 nm), and a long pass (590 nm) barrier filter. Photomicrography was performed at ×200 with commercial color print film‖ and timed exposures (60–90 sec, typically).

The luminescence properties of Eu and other lanthanide complexes are well described in the chemistry literature [22]. Excitation of outer-shell electrons may be produced by UV or laser-generated visible light (Fig. 3). Excitation to the $^5D_2$ state in this example is followed by rapid (<5 μsec) radiationless transition to the luminescent $^5D_0$ state. Emission to the ground ^7F manifold from the $^5D_0$ state results in a characteristic spectrum of orange-red lines (Fig. 3).

In a preliminary experiment, crystalline Eu-DTPA was prepared as described above and placed on a glass slide with coverslip. Red-range fluorescence was easily observed (Fig. 4). A visually indistinguishable fluorescence pattern was detected from Eu_2O_3 crystals, implying no significant interference from the DTPA ligand. By contrast, neither Gd_2O_3 nor Gd-DTPA crystals were observed to fluoresce in this system.

To determine the visible threshold for the detection of Eu-DTPA in our system, a dilution experiment was performed. Cubes of rat brain weighing approximately 1 mg each were freshly harvested and soaked for 10 min in various concentrations of Eu-DTPA (10–500 mmol/l). The specimens were then removed from solution and air-dried on a glass slide for 30 min. Eu-DTPA luminescence could be visibly detected in our system at concentrations of the soaking solution as low as 50 mmol/l. While we do not know the resultant Eu-DTPA concentration present inside each cube of soaked tissue, we may presume it was no greater than that of the soaking solution. On the basis of this assumption we may conclude that a reasonable upper limit for the minimum concentration of Eu-DTPA visibly detectable by our fluorescence microscope system was 50 mmol/l, or approximately 0.05 mmol/g of tissue.

* Eu_2O_3, Aldrich Chemical Company, Milwaukee, WI.
† H_5-DTPA, Aldrich.
‡ Magnevist, Berlex Imaging, Cedar Knolls, NJ.
§ Zeiss, West Germany.
‖ Kodacolor, ASA 400.

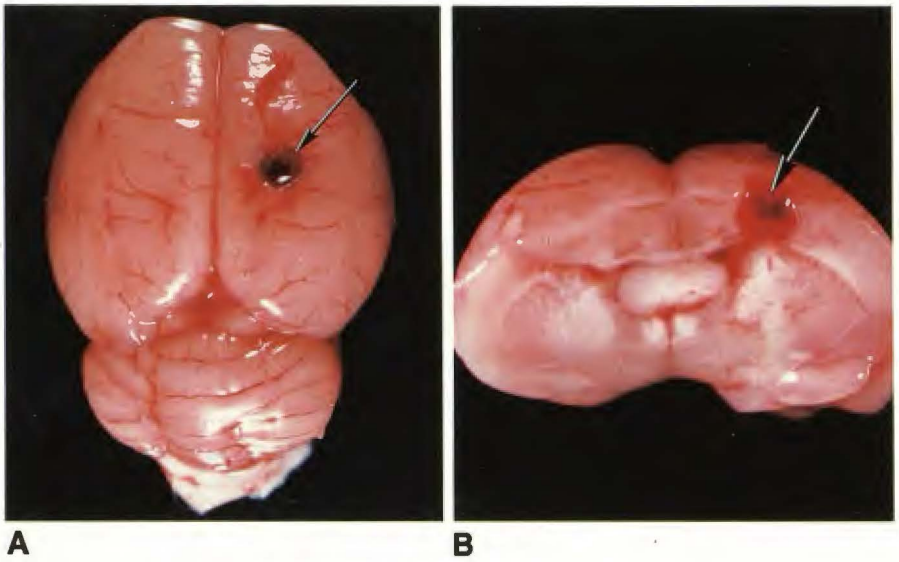

Fig. 1.—Experimental brain laceration in the rat.

***A*, Superior view of whole rat brain shows site of injury (*arrow*) in posterior right frontal lobe.**

***B*, Coronal section through frontal lobes at level of laceration (*arrow*) shows local hemorrhage but relatively little surrounding brain injury.**

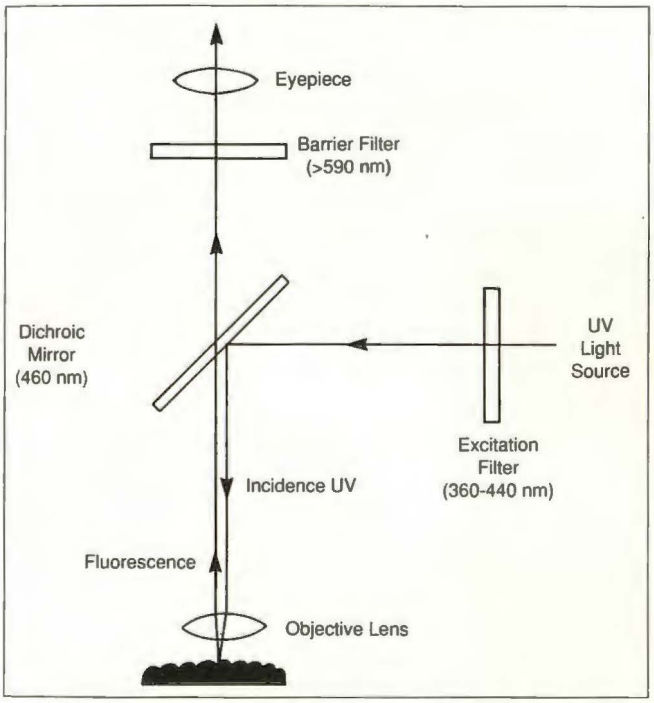

Fig. 2.—Diagram showing arrangement of filters and lenses in a fluorescence microscope. Numbers in parentheses under each filter indicate the wavelengths of light allowed to pass.

Electron Probe Microanalysis

Electron probe microanalysis of crystals and tissue specimens was performed on a commercially available system.[¶] A 25 kV accelerating voltage was used on all specimens with a working distance of 15 mm in the scanning fast raster mode (magnification ×500). Spectral peaks were acquired for 90–120 sec and analyzed on a Tracor Northern EDXA 5500 system.[**]

Electron probe microanalysis (energy dispersive X-ray spectroscopy, EDX) is a relatively new electron microscopic technique allowing the identification of specific elements with an atomic number greater than 9. Several detailed reviews of the physical principles underlying this technology are available [28–31]. In EDX, electrons serve as an excitation source and bombard a sample tissue. These electrons dislodge resident electrons in inner orbitals of the specimen atoms. Characteristic X-rays are then emitted by the histologic sample, a process identical to that which occurs in conventional X-ray tubes. The characteristic radiation is detected by a field-effect transistor and can be definitively assigned to a specific element.

In the low-voltage (25 kV) electron microscopy used here, the characteristic radiation lines of Gd and Eu recorded come primarily from L shell emissions [32]. The critical absorption and emission energies for Gd and Eu are significantly different so that each may be detected (Fig. 5, Table 2).

Tissue specimens analyzed with EDX were freshly frozen and then freeze-dried. Small cubes of tissue from target areas (kidney, pituitary, etc.) measuring approximately 1 mm^3 were first flash-frozen by dipping them in liquid nitrogen for 45 sec. The frozen tissues were then transferred to a freeze-drying apparatus[††] initially cooled to −50°C with thawing and dehydration of tissue samples over a 24-hr period. The dried specimens were mounted on grids and then carbon-coated for electron microscopy and X-ray spectroscopic analysis.

A dilution experiment to determine minimal detectable concentrations of Eu-DTPA and Gd-DTPA in freeze-dried rat brain was undertaken, similar to that described for detecting Eu-DTPA by fluorescence microscopy. Cubes of rat brain (approximately 1 mg size) were soaked for 10 min in various concentrations of Eu-DTPA and Gd-DTPA (1–500 mmol/l), then flash-frozen and freeze-dried. EDX spectra were plotted. In our system it was determined that the threshold for reliable detection of Gd-DTPA and Eu-DTPA was approximately 5 mmol/l (0.005 mmol/g tissue). The EDX system was therefore an order of magnitude more sensitive than fluorescence microscopy for detecting Eu-DTPA in brain specimens.

Results

Gd-DTPA and Eu-DTPA were easily detected in most tissue samples studied by EDX (Table 3). Characteristic X-ray peaks

[¶] Hitachi H-600 scanning electron microscope equipped with backscattered electron and X-ray detectors.

[**] Tracor Northern, Inc., Middleton, WI.

[††] Labconco Freeze Dry 5, Kansas City, MO.

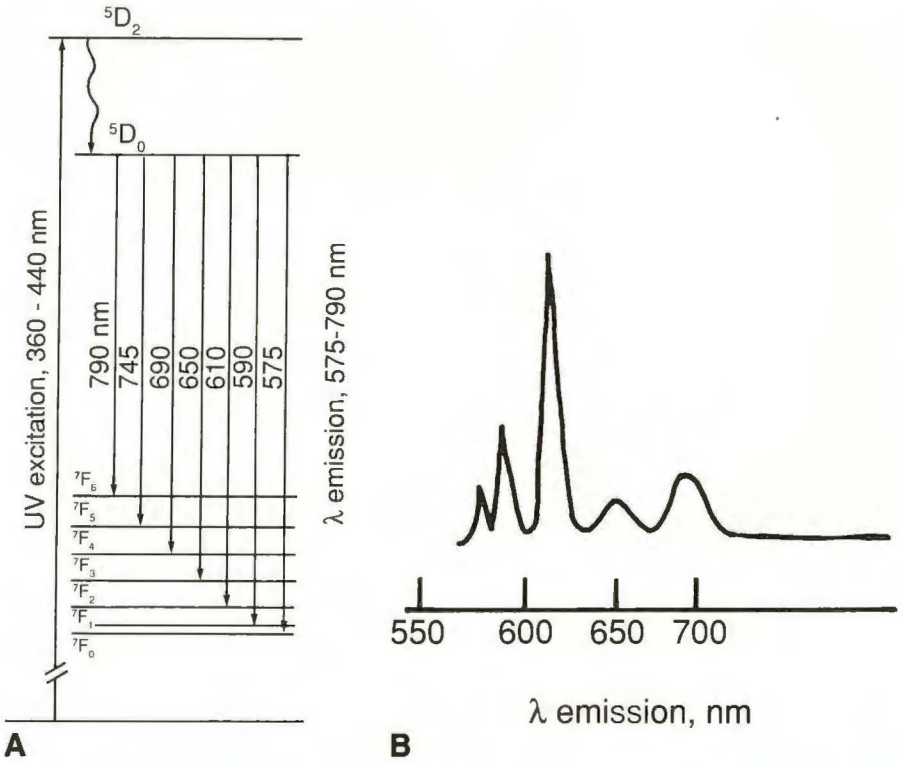

Fig. 3.—Fluorescence–excitation scheme for europium (III) complexes. (Adapted from [26].)

***A*, Electron transition map for fluorescence. UV excitation carries electron energy to the $^5D_2$ state. Rapid (<5 μsec) nonradioactive relaxation to the luminescent $^5D_0$ state follows. Emission to the ground ^7F manifold results in fluorescent emission of light (575–790 nm).**

***B*, The fluorescence spectrum of europium (III) corresponding to decay to the ^7F energy levels. The array of wavelengths results in an orange-red visible luminescence.**

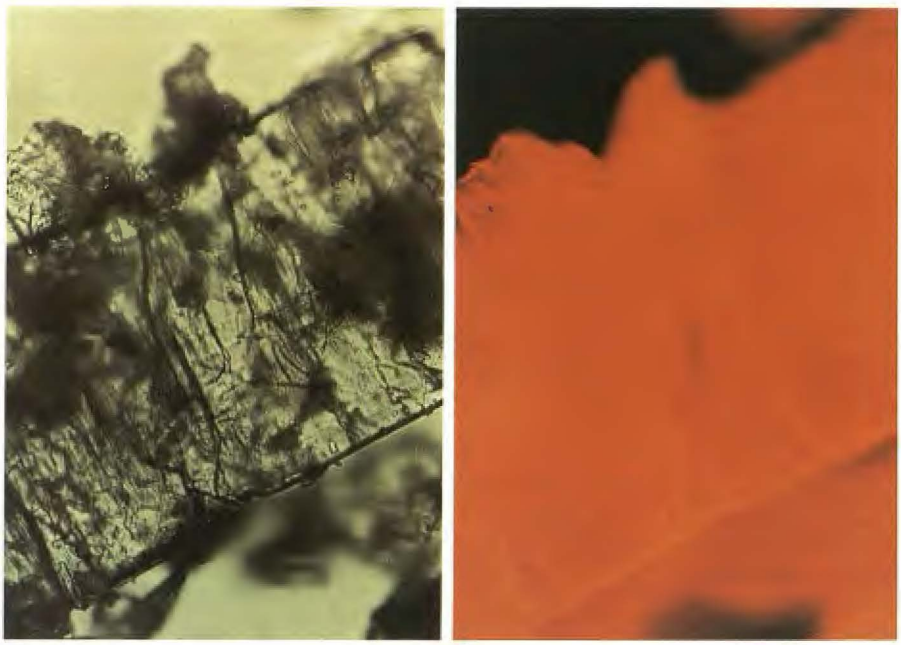

Fig. 4.—*A* and *B*, Light transmission (*A*) and incident UV light epifluorescence (*B*) images of Eu-DTPA crystals. Note distinct orange-red fluorescence of the crystals in *B*.

were most readily detected in those organs known to concentrate the agents, especially those of the abdominal viscera [19]. Intracranially, Gd and Eu spectra were detected only in those areas known to lie outside the blood-brain barrier: dura, pituitary, and choroid plexus. Equivocal or trace spectra were recorded from the optic nerves.

Neither Gd-DTPA nor Eu-DTPA apparently crossed an intact blood-brain barrier, since no Gd or Eu spectra were detected in the normal pons, cerebrum, or cerebellum. In those rat brains injured by laceration 1 hr prior to injection, however, both Gd and Eu were detected immediately near the site of injury. Neither Gd nor Eu was detected in the white matter within 5 mm of the lesion, suggesting that little diffusion of contrast material occurred in this particular brain injury model.

No Gd or Eu peaks were detected in control rats injected

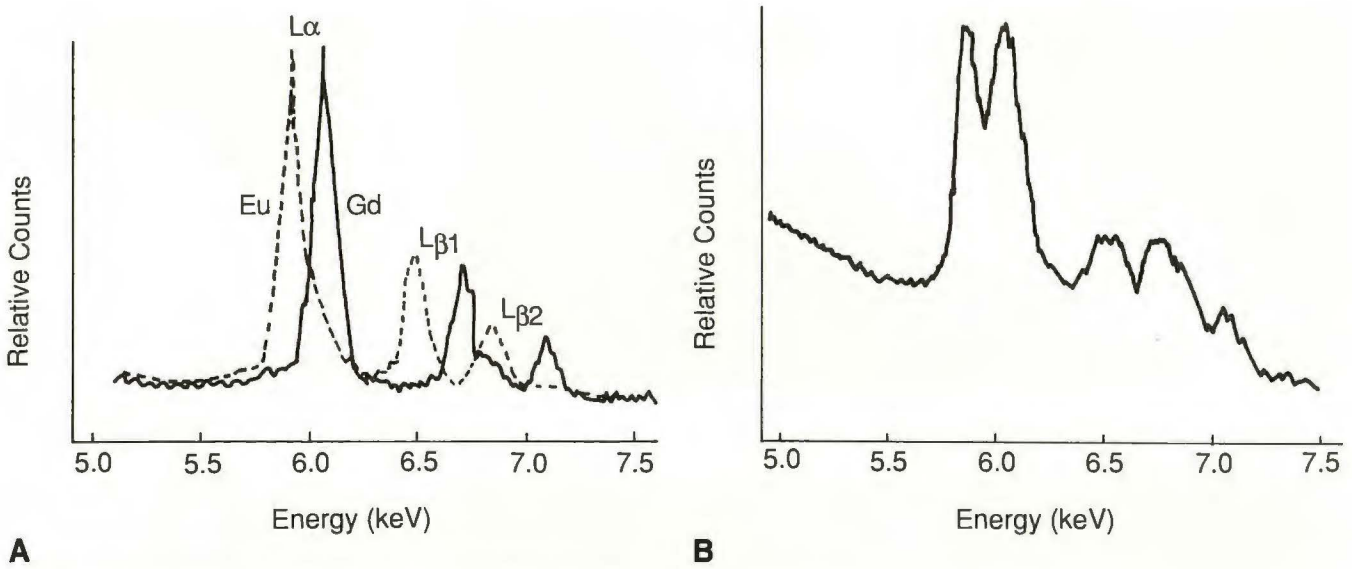

Fig. 5.—L-characteristic radiation of Eu and Gd from soaked tissue.

***A*, Tracing of EDX analysis printout shows characteristic peaks for individual samples of Eu (*dotted line*) and Gd (*solid line*). The Lα, $L\beta_1$, and $L\beta_2$ peaks were most easily identified.**

***B*, EDX spectrum from tissue containing both Eu and Gd. Because of scattering effects and the relatively close energies of L-characteristic radiations, peaks for each element overlap to a variable degree. Even with overlap the combined spectral pattern was thought sufficiently unique from that possessed by either element alone that their joint presence in a sample could be reliably determined.**

TABLE 2: Principal X Ray Critical Absorption and Emission Energies (keV)

Element	Emission Band				
	$\bar{M}\alpha$	$L\alpha_1$	$L\beta_1$	$L\beta_2$	$\bar{K}\alpha$
Eu	1.13	5.85	6.49	6.84	41.32
Gd	1.19	6.06	6.72	7.10	42.76

with saline. In rats injected both with Gd-DTPA and Eu-DTPA, a parallel presence or absence of Gd- and Eu-spectra was noted in the tissues. The above findings support our hypothesis that Eu-DTPA and Gd-DTPA distribute identically both in normal and injured tissues.

Eu-DTPA was observed by fluorescence microscopy in the same areas in which EDX analysis showed it to be accumulated (Table 4). The highest fluorescence intensities were seen in the kidney (Fig. 6), liver, and choroid plexus (Fig. 7). In general, the fluorescence observed was not localized to particular cells or vessels. This finding is consistent with the known broad extracellular distribution of DTPA compounds within their target organs.

In some areas known to enhance vividly with contrast material (e.g., spleen, pituitary), EDX spectra confirmed the presence of Eu and Gd, but Eu fluorescence was very weak. It is uncertain whether the concentration of Eu in these tissues was merely near the threshold for detection or whether unknown tissue factors such as interactions with proteins or calcium quenched the luminescence spectra in these regions.

No luminescence could be detected in the blood itself nor in intact brain regions beyond the blood-brain barrier. In animals injured experimentally, local contrast accumulation at the laceration site could be detected by both EDX and fluorescence microscopy (Fig. 8). In this case, Eu-DTPA appeared

TABLE 3: Detection of Eu and Gd EDX Spectra in Rat Tissues After Various Intravascular Injections

Tissue	Injection		
	Gd-DTPA	Eu-DTPA	Gd-DTPA + Eu-DTPA
Liver	Gd	Eu	Gd + Eu
Spleen	Gd	Eu	Gd + Eu
Skeletal muscle	Gd	Eu	Gd + Eu
Kidney	Gd	Eu	Gd + Eu
Dura	Gd	Eu	Gd + Eu
Choroid	Gd	Eu	Gd + Eu
Pituitary	Gd	Eu	Gd + Eu
Optic nerve	?Gd	?Eu	?Gd + ?Eu
Pons	–	–	–
Frontal lobe	–	–	–
Cerebellum	–	–	–
Laceration site	Gd	Eu	Gd + Eu

Note.—After intravascular injection of saline, neither Gd nor Eu was detected in any of the tissues. Question mark means equivocal or trace spectra were recorded.

TABLE 4: Visible Fluorescence of Eu-DTPA in Rat Tissues

Tissue	Luminescence Observed
Liver	Bright
Spleen	Weak
Skeletal muscle	Weak
Kidney	Bright
Dura	Moderate
Choroid plexus	Bright
Pituitary	Weak
Optic nerve	None
Pons	None
Frontal lobe	None
Cerebellum	None
Laceration site	Weak

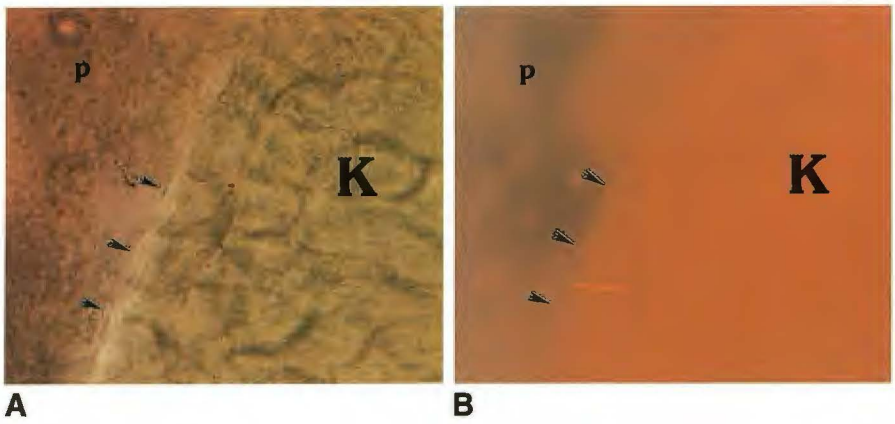

Fig. 6.—*A* and *B*, Light transmission (*A*) and UV epifluorescence (*B*) images at edge of rat kidney (K). The renal capsule is marked by *arrowheads*. Diffuse luminscence within kidney is noted. Some leakage of luminescent blood and urine as a result of sectioning in the perirenal space (p) is also observed. (Unstained, ×280)

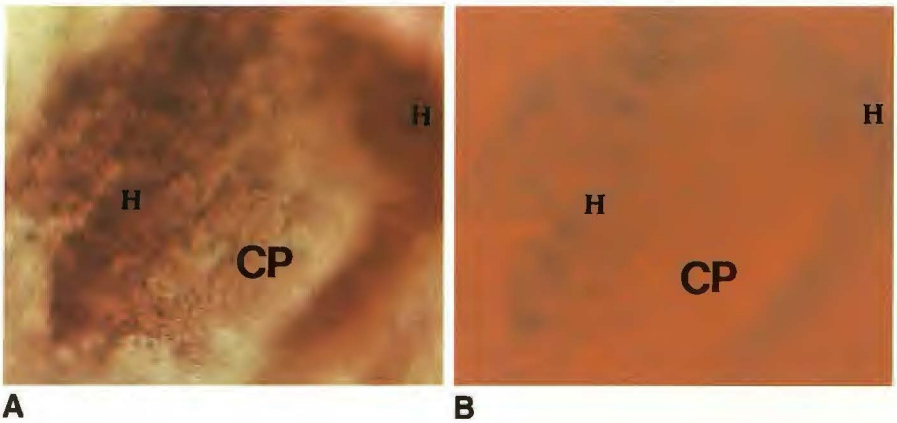

Fig. 7.—*A* and *B*, Light transmission (*A*) and UV epifluorescence (*B*) image of rat choroid plexus (CP). The section of specimen chosen for this illustration contains appreciable areas of hemorrhage (H). Strong orange-red luminescence is noted throughout most of the specimen in *B*. Little fluorescence in the hemorrhagic areas is observed, possibly because they contain densely packed red blood cells and little serum-containing Eu-DTPA. Despite rapid removal of this specimen, considerable autolysis has occurred. (×200)

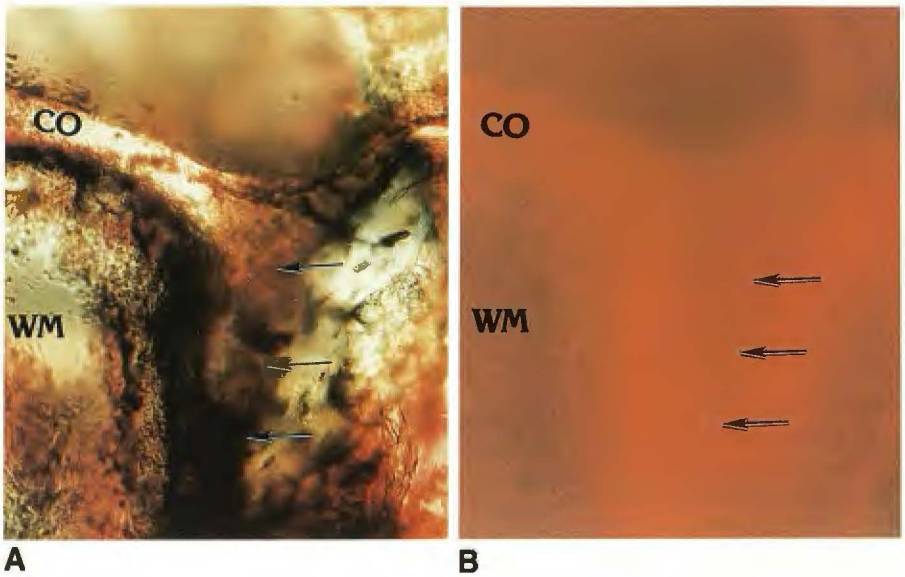

Fig. 8.—*A* and *B*, Light transmission (*A*) and epifluorescence (*B*) images of rat brain at margin of experimental laceration (*arrows*). Cerebral cortex (CO) and subcortical white matter (WM) are noted. Intense luminescence of Eu-DTPA is seen in *B* along margins of laceration. Fluorescence of cortex adjacent to laceration is also noted. (×100)

to coat the edges of the laceration and spill over onto the adjacent cortex. It is unclear whether this represented leakage of contrast material from the laceration edges with diffusion into surrounding brain or direct local leakage of contrast material into marginally injured brain.

Discussion

The recent development of MR contrast agents has ushered in an exciting new era of opportunities for research and for improved patient care. Gd-DTPA, the first of these agents

to be widely used, has already proved itself of great clinical benefit in a number of disease states [1–11]. Although clinically oriented knowledge about these compounds is rapidly proliferating, much remains to be learned about their accumulation, transport, and dynamics at the microscopic level.

It has been generally assumed that soluble contrast agents used in CT, MR, and nuclear medicine behave similarly: they do not cross an intact blood-brain barrier and distribute in the extracellular spaces around lesions [12–23]. While this view is correct as a first approximation, many unanswered questions remain. Do contrast agents penetrate neoplastic cells? To what extent is contrast enhancement due to tumor vascularity, accumulation in tumor interstitial fluid, or direct leakage from tumor capillaries? Do CT and MR contrast agents distribute identically or only similarly?

The predominant extracellular location and extreme solubility of most radiologic agents make their precise localization in tissue difficult. Traditional methods of tissue fixation for microscopy or autoradiography can significantly dislocate these compounds or wash them completely from the specimen [24, 25]. Either flash-frozen or rapidly analyzed fresh tissue must be used to avoid major shifts of these soluble substances between tissue compartments.

Several other sophisticated techniques for detecting and quantifying Gd in tissue specimens exist [32–34]. Inductively coupled plasma (ICP) atomic emission spectroscopy is the most sensitive method, being capable of detecting Gd in concentrations as low as 1 μM [32]. Polarized X-ray fluorescence excitation analysis (FEM) is slightly less sensitive than ICP, but can still detect Gd or Eu in the parts per million (ppm) range [33]. High-performance liquid chromatography (HPLC) is a practical and economic alternative for quantification of Gd or Eu, with a sensitivity of about 20 ppm [32].

The EDX and fluorescent microscopic (FM) techniques reported here are several orders of magnitude less sensitive than ICP, FEA, and HPLC. However, it should be emphasized that these latter techniques are wholly analytical and require destruction of the tissue sample in order to be implemented. The EDX and fluorescent techniques, while much less sensitive, allow for preservation of tissue morphology. EDX and FM should not be thought of as competing quantitative assays, therefore, but rather as new methods for localizing Gd or Eu in tissues at the microscopic level.

We report here the development of an analogue of Gd-DTPA that can be directly detected at the level of the light microscope. Eu-DTPA is suitable for this purpose for several reasons. First, Eu and Gd are neighboring elements on the periodic table, have the same valences, and have similar ionic radii and atomic weights [35]. We would presume, therefore, that the tissue distributions of Gd-DTPA and Eu-DTPA would be nearly identical, a result supported by our EDX analysis. The luminescence properties of Eu are well known to chemists and physicists who study the lanthanide elements [26]. The red-range phosphorescence of Eu is also familiar to television engineers; Eu-based complexes are used as the red phosphors in many color TV picture tubes [36].

Our research has documented the validity and feasibility of using Eu compounds as fluorescent analogues for Gd. We have demonstrated that one can visualize the red luminescence of Eu-DTPA in unfixed tissue specimens by using a general purpose fluorescent microscope with the filters we have described. Further research in our method will be aimed in two directions: (1) optimizing microscopic techniques for fluorescence excitation and recording, and (2) improving methods for tissue preparation and preservation.

To improve the microscopic images, we are currently exploring several options. The efficiency of fluorescence excitation can be improved by the installation of quartz-based optics and a lower pass excitation filter. This would allow stimulation of the specimen with higher energy UV photons (i.e., those with wavelengths less than 340 nm). The ideal system, although admittedly expensive, would employ excitation of the specimen with a high energy pulsed dye laser. Monochromatic photons at 465 nm have been shown optimal for inducing transitions of Eu (III) electrons to excited states [26]. Such a system would likely be capable of generating the maximal fluorescence possible from a given specimen.

The fluorescence detection methods can be improved greatly by employing a low-level light detector, such as silicon target cameras in combination with video-enhancing image processing [37, 38]. This technique employs signal averaging to extract the presence of very weak fluorescences from background noise. This method will allow the use of higher magnification and the detection of significantly lower levels of fluorescence in tissues.

The full application of our model to a variety of pathologic lesions will require significant improvements in our techniques of tissue preparation. Acceptable results may be obtained by viewing rapidly harvested and freshly mounted tissue. However, some of our specimens demonstrated significant autolysis even in the 5–10 min required to set up the microscope. Since Gd-DTPA would easily be washed from tissue by traditional methods of tissue fixation, the most logical solution would be to perform frozen sectioning of tissue and view the specimens on a fluorescent microscope fitted with a cold stage. Such a technique would not only preserve the tissues under study but minimize translocation of the very soluble extracellular Eu-DTPA.

We are also currently exploring the use of terbium(Tb)-DTPA as another fluorescent analogue for Gd-DTPA. Our preliminary data suggest that Tb compounds may be far superior to those of Eu. Tb compounds possess a blue-green fluorescence under UV excitation, which is an order of magnitude brighter than that emitted by Eu. Photographic exposure times can be reduced from minutes to seconds by using Tb-DTPA instead of Eu-DTPA.

Conclusions

In summary, we have demonstrated a creative, new approach for investigating the distribution and dynamics of Gd-based contrast agents at the microscopic level. We have shown the feasibility and validity of using Eu analogues of Gd, and have synthesized and tested one such compound (Eu-DTPA). We have demonstrated that Eu-DTPA can be reliably detected in tissues by its characteristic luminescence

when exposed to UV light, and that this compound distributes in parallel with Gd-DTPA. Possible future refinements in our experimental techniques should allow better detection and localization of Eu-DTPA in cells and tissues.

The outstanding clinical success recently enjoyed by Gd-DTPA has guaranteed a secure future both for itself and for newer MR contrast agents. However, complete appreciation of how these agents affect the MR image will not be attained until we more fully understand their distribution, diffusion, and accumulation at the cellular level. The research presented here represents a successful first attempt to attack this problem. The intelligent design of future agents that are tissue-, pH-, or pathology-specific demands that the spirit of such work continues.

REFERENCES

1. Breger RK, Papke RA, Pojunas KW, Haughton VM, Williams AL, Daniels DL. Benign extraaxial tumors: contrast enhancement with Gd-DTPA. *Radiology* **1987**;163:427–429
2. Brant-Zawadzki M, Berry I, Osaki L, et al. Gd-DTPA in clinical MR of the brain: 1. Intraaxial lesions. *AJNR* **1986**;7:781–788, *AJR* **1986**;147:1223–1230
3. Berry I, Brant-Zawadzki M, Osaki L, et al. Gd-DTPA in clinical MR of the brain: 2. Extraaxial lesions and normal structures. *AJNR* **1986**;7:789–793, *AJR* **1986**; 147:1231–1235
4. Healy ME, Hesselink JR, Press GA, Middleton MS. Increased detection of intracranial metastases with intravenous Gd-DTPA. *Radiology* **1987**;165: 619–624
5. Felix R, Schorner W, Laniado M, et al. Brain tumors: MR imaging with gadolinium-DTPA. *Radiology* **1985**;156:681–688
6. Haughton VM, Rimm AA, Czervionke LF, et al. Sensitivity of Gd-DTPA–enhanced MR imaging of benign extraaxial tumors. *Radiology* **1988**; 166:829–833
7. Grossman RI, Gonzalez-Scarano F, Atlas SW, Galetta S, Silberberg DH. Multiple sclerosis: gadolinium enhancement in MR imaging. *Radiology* **1986**;161:721–725
8. Grossman RI, Joseph PM, Wolf G, et al. Experimental intracranial septic infarction: magnetic resonance enhancement. *Radiology* **1985**;155: 649–653
9. Sze G. Gadolinium-DTPA in spinal disease. *Radiol Clin North Am* **1988**;26: 1009–1024
10. Grossman RI, Braffman BH, Brorson JR, et al. Multiple sclerosis: serial study of gadolinium-enhanced MR imaging. *Radiology* **1988**;169:117–122
11. Russell EJ, Geremia GK, Johnson CE, et al. Multiple cerebral metastases: detectability with Gd-DTPA–enhanced MR imaging. *Radiology* **1987**;165: 609–617
12. Gado MH, Phelps ME, Coleman RE. An extravascular component of contrast enhancement in cranial computed tomography. Part I. The tissue-blood ratio of contrast enhancement. *Radiology* **1975**;117:589–593
13. Gado MH, Phelps ME, Coleman RE. An extravascular component of contrast enhancement in cranial computed tomography. Part II. Contrast-enhancement and the blood-tissue barrier. *Radiology* **1975**;117:595–597
14. Sage MR. Kinetics of water-soluble contrast media in the central nervous system. *AJR* **1983**;141:815–824
15. Dean PB, Kormano M. Intravenous bolus of ^{125}I labeled meglumine diatrizoate. Early extravascular distribution. *Acta Radiol [Diagn]* (Stockh) **1977**;18:293–304
16. Haynie TP, Konikowski T, Glenn HJ. The kinetics of ^{99m}Tc-, ^{113m}In- and ^{169}Yb-DTPA compounds in brain sarcoma and kidneys of mice. *J Nucl Med* **1972**;13:205–210
17. Tutor CH. Radiopharmaceuticals for tumor localization with special emphasis on brain tumors. In: Subramanian G, Rhodes BA, Cooper JF, Sodd VJ, eds. *Radiopharmaceuticals*. New York: Society of Nuclear Medicine, **1975**:474–481
18. Raimondi AJ. Localization of radio-iodinated serum albumin in human glioma. An electron-microscopic study. *Arch Neurol* **1964**;11:173–184
19. Strich G, Hagan PL, Gerber KH, Slutsky RA. Tissue distribution and magnetic resonance spin lattice relaxation effects of gadolinium-DTPA. *Radiology* **1985**;154:723–726
20. Allard M, Kieu P, Caille JM, Bonnemain B, Doucet D, Simonnet G. Subcellular localization of gadolinium in the rat brain. *J Neuroradiol* **1987**;14: 159–162
21. Prato FS, Wisenberg G, Marshall TP, Vksik P, Zabel P. Comparison of the biodistribution of gadolinium-153 DTPA and technetium-99m DTPA in rats. *J Nucl Med* **1988**;29:1683–1687
22. Barnhardt JL, Kuhnert N, Bakam DA, Berk RN. Biodistribution of $GdCl_3$ and Gd-DTPA and their influence on proton magnetic relaxation in rat tissue. *Magn Reson Imaging* **1987**;5:221–231
23. Wolman M, Klatzo I, Chui E, et al. Evaluation of the dye-protein tracers in pathophysiology of the blood-brain barrier. *Acta Neuropathol* **1981**;54: 55–61
24. Roth LJ, Stumpf WE. *Autoradiography of diffusible substances*. New York: Academic Press, **1969**:69–80
25. Rogers AW. *Technique of autoradiography*. Amsterdam: Elsevier, **1979**: 153–182
26. Horrocks WD Jr, Sudnick DR. Lanthanide ion probes of structure in biology. Laser-induced luminescence decay constants provide a direct measure of the number of metal-coordinated water molecules. *J Am Chem Soc* **1978**;101:334–338
27. Weinmann HJ, Brasch RC, Press WR, Wesbey GE. Characteristics of gadolinium-DTPA complex: a potential NMR contrast agent. *AJR* **1984**; 142:619–624
28. Suzuki S, Kitajima H. Energy dispersive x-ray spectroscopy in medium voltage electron microscope. *J Electron Microsc (Tokyo)*. **1987**;35: 335–342
29. Shuman H, Somlyo AV, Somlyo AP. Quantitative electron probe microanalysis of biological thin sections: methods and validity. *Ultramicroscopy* **1976**;1:317–339
30. Heyman RV, Sauberman AJ. Multifunctional minicomputer program providing quantitative and digital x-ray microanalysis of cryosectioned biological tissue for the inexperienced analyst. *J Electron Microsc Tech* **1987**;5: 315–345
31. Gorlen KE, Barden LK, Del Priore JS, Fiori CE, Gibson CC, Leapman RD. Computerized analytical electron microscope for elemental imaging. *Rev Sci Instrum* **1984**;55:912–921
32. Weinmann HJ, Laniado M, Mutzel W. Pharmacokinetics of Gd DTPA/dimeglumine after intravenous injection into healthy volunteers. *Physiol Chem Phys Med NMR* **1984**;16:167–172
33. Wang S, Morita U, White DL, Kaufman L, Brasch RC. MR image enhancement as a function of tissue gadolinium concentration, measured with polarized x-ray fluorescence analysis. *Radiology* **1988**;169(P):40
34. Elster AD. Use of energy dispersive x-ray (EDX) microscopy to trace gadolinium in tissues. *Radiology* **1989**; (in press)
35. Weast RC, Astle MJ, eds. *CRC handbook of chemistry and physics*, 62nd ed. Boca Raton, FL: CRC Press, **1982**
36. Grob B. *Basic television principles and servicing*, 4th ed. New York: McGraw-Hill, **1975**
37. Allen RD, Allen NS. Video-enhanced microscopy with a computer frame memory. *J Microsc* **1983**;129:3–17
38. Inoue S. *Video microscopy*. New York: Plenum Press, **1986**